Pertanika J. Sci. & Technol. 29 (4): 3113 - 3141 (2021)

PERTANIKA JOURNALS

SCIENCE & TECHNOLOGY

Journal homepage: http://www.pertanika.upm.edu.my/

Optimisation Design of Functionally Graded Sandwich Plate with Porous Metal Core for Buckling Characterisations

Emad Kadum Njim[1]*, Sadeq Hussein Bakhy[1] and Muhannad Al-Waily[2]

[1] *University of Technology, Mechanical Engineering Department, Baghdad, 10066 Iraq*
[2] *University of Kufa, Faculty of Engineering, Mechanical Engineering Department, Najaf, 54001 Iraq*

ABSTRACT

This study presents the optimum operating parameters and geometrical of the functionally graded sandwich plate with porous materials (FGPMs), widely used in aircraft structures subjected to uniaxial critical buckling load. This process is developed design optimisation parameters by employing Multi-Objective Genetic Algorithm (MOGA) techniques. According to a simple power law, the assumption of varying material characteristics of the porous FG core through the plate thickness is considered. In addition, to evaluate the linear buckling behaviour, a new mathematical model based on the classical plate theory (CPT) is proposed. The impact of different design parameters on the performance of the functionally graded structure is studied. Then, finite element modelling is used to validate the results of the analytical solution. Finally, the optimisation method includes both design of experiments (DOE) and response surface methodology (RSM), which are used to find out the critical buckling load of the FG sandwich plate with porous metal core bonded with two homogenous skins using suitable adhesion. The mandatory constraints are the maximum critical buckling and maximum total deformation. In this work, 100 design points are considered to determine the total deformation load multiplier, maximum deformation, and equivalent stress of sandwich plate with graded materials and even distribution of porosities. The buckling analyses of the FGPM sandwich plate subjected to the compression loading are presented by conducting an experimental program. The results show good convergence

ARTICLE INFO

Article history:
Received: 2 June 2021
Accepted: 30 July 2021
Published: 28 October 2021

DOI: https://doi.org/10.47836/pjst.29.4.47

E-mail addresses:
emad.njim@gmail.com (Emad Kadum Njim)
20093@uotechnology.edu.iq (Sadeq Hussein Bakhy)
muhanedl.alwaeli@uokufa.edu.iq (Muhannad Al-Waily)
*Corresponding author

ISSN: 0128-7680
e-ISSN: 2231-8526

between suggested analytical and FEA simulation with an average error percentage of no more than 2 %.

Keywords: Classical plate theory, critical buckling load, DOE, FEA, FGPMs, mathematical model, optimisation, RMS

INTRODUCTION

Functionally graded materials (FGMs) are known as new advanced materials can achieve higher performance by mixing two or more completely different components, the volume fraction of which is gradually changed in one or more directions, and combined with the required material properties, thus reducing the stress concentration found in laminated composites (Emad et al., 2021a). Due to the ability to produce materials with tailor-made properties, this material is suitable for various important applications, such as energy, aerospace, automobile, defence, marine, and biomedical, so people's interest in FGM is increasing. In addition, many researchers have been studying various aspects of static, vibration, buckling, and design (Bassiouny et al., 2020). The most popular FGMs are metal-ceramic constituents, usually showing a power-law distribution to describe their material properties.

In most fabrication processes, microvoids and porous may be found in the FGM structure leading to compatibility reduction of materials (Zhao et al., 2019). FGM structures with porous materials are essential and have unique attributes in many industrial and biomedical applications (Emad et al., 2021b). The classical plate theory (CPT) of sandwich structure is proposed considering the interrupted line hypothesis. A further improvement of this theory is considering the thin layer that combines the surface and the core (Krzysztof & Ewa, 2021). Numerous studies have been published in the literature on the stability analysis of functionally graded sandwich structures.

To predict the imperfect FGM sandwich plate's performance in post-buckling using in-plane mechanical compression load, Vuong and Chin (2018) introduced the concept of high-order shear deformation and the FEA meshfree method in their solution. They concluded that loading type and geometrical properties influence the stability of the FGM structure. Hessameddin and Farid (2020) investigated buckling characteristics of sandwich plates with different boundary conditions and proposed mathematical formulations according to modified shear deformation theory. They examined the sandwich plate performance against linear buckling by taking the effect of some input parameters and employing a response surface methodology (RSM) in their analysis. D. Chen et al. (2019) used the Chebyshev-Ritz method to study bending and buckling analyses of the FG plate with a different arrangement of porosity distribution. The results show that the proposed porous model can reduced interfacial failure and improved buckling and bending performances.

The buckling behaviours of a functional graded polymeric sandwich plate subjected to different load cases have been presented by Mine and Uğur (2020). Moreover, Abo-Bakr et al. (2021) used variable axial load conditions to investigate optimal weight for buckling loads of the two constituents functionally graded beams with volume fraction following the sigmoid function. Z. Chen et al. (2019) studied the flexural buckling problems of the FGMs sandwich structure considering thermal-induced non-uniform cross-sectional properties and taking into accounts the influence of transverse shear deformation. Michele (2020) analysed the impact of the uneven arrangement of the core-oriented fibres using various materials on buckling loads of functionally graded orthotropic plates. J. F. Wang et al. (2021) introduced the meshless method and discussed a composite quadrilateral plate's stability and thermal vibration features with the FG carbon reinforced with a nanotube. Yassir et al. (2021) proposed a high-order mathematical model to examine stability analysis of the FG plate structure using the finite element method. Recently, many important studies have been published and discussed the development and design problems of FGMs (Mrinal & Manish, 2021; Nikbakht et al., 2019; Yi et al., 2019). A comprehensive study in optimisation shape and material for stability and performance behaviour of functionally graded toroidal shells has been conducted by Thang et al. (2020).

C. Wang et al. (2021) presented an optimisation process to improve the performance of piezoelectric FG plates by analysing shape control using a multi-objective isogeometric integrated method. Jin and Masatoshi (2015) worked on minimising the flexibility of FG sandwich structures by conduct a reliable design and optimisation analysis using an interface shape method, taking into accounts the volume constraints of the FG part. Zhu et al. (2009) presented an optimal study of sandwich panels under impact loading conditions to study the buckling behaviour considering the effect of different design parameters. Additionally, to solve the stability problem of functionally graded plates work in a thermal environment and under the influence of mechanical loadings, multi-objective design optimisation is conducted by Moleiro et al. (2020). In order to generate a design of lightweight structures based on prospective yield performance, Bai et al. (2019) presented a new approach of topology optimisation considering maximum applied stress as a constraint to design graded lattice structures. According to the literature, many scientists have adopted great attention to study the static, dynamic, and stability problems of FGM structure. However, many limitations are still present and need further study. For example, the comprehensive study of eigenvalue buckling, design, and optimisation of FGM imperfect sandwich plate follow power-law variation by applying in-plane loads has not been studied previously.

The current study presents a linear buckling analysis of simply-supported FG sandwich plates with uniform porosity distribution. The mathematical formulations are developed by using the classical thin plate theory. In accordance with this aim, total deformation and critical stresses are obtained for various geometrical considerations. Many important

design parameters, such as porosity ratio, volume fraction index, and thickness ratio, are considered in detail–numerical results obtained by Ansys test the accuracy and validity of the proposed analytical solution. A new optimisation analysis using the concept of design of experiments (DOE) and Response Surface Method (RSM) are carried out to evaluate the stability characteristics of the FG sandwich plate with porous metal. The number of design points considered is 100. The chosen design variables include porosity ratio (Beta), gradient index (k), and core thickness (h), as while the Total Deformation, Equivalent Stress, and Total Deformation Load Multiplier are chosen as response functions. The ranges of the input variables considered in this study are porosity factor ($Beta$= 0-0.5), volume fraction index (k= 0-5), thickness of face sheet (h_1=2-2.5) mm, and FG core height (h= 5-25) mm. Moreover, to approximate the results, a dxrom software is combined with ANSYS DesignXplorer is presented. The main contribution of this work is that the paper reports a comprehensive study of the porous FGM material and provides useful analysis and results, which would be helpful for the usage of such materials in the engineering industry. The results obtained may encourage many researchers to conduct further works on porous FG sandwich structures.

MATERIALS AND METHOD

Consider the model of a supported, rectangular FGM plate with cartesian coordinates (x, y, z), composed of two constituents (Al_2O_3/Al) core bonded at top and bottom surfaces with isotropic metal skin as shown in Figure 1. The width a, length b, and total thickness h are the main dimensions of the plate. The plate is subjected to uniaxial force F_x acting on the plate boundaries along the x-direction. According to classical plate theory, the stress-strain relation for the FG plate is given by Equations 1a, 1b, and 1c (Phi et al., 2021; Arefi & Najafitabar, 2021),

$$\sigma_x = -\frac{Ez}{1-v^2}\left(\frac{\partial^2 w}{\partial x^2} + v\frac{\partial^2 w}{\partial y^2}\right) \quad [1a]$$

$$\sigma_y = -\frac{Ez}{1-v^2}\left(\frac{\partial^2 w}{\partial y^2} + v\frac{\partial^2 w}{\partial x^2}\right) \quad [1b]$$

$$\tau_{xy} = -\frac{Ez}{(1+v)}\frac{\partial^2 w}{\partial x \partial y} \quad [1c]$$

Similarly, the corresponding moment resultants components M_x, M_y, and M_{xy} respectively can also be given as Equations 2, 3a, 3b, and 3c:

$$\begin{Bmatrix} M_x \\ M_y \\ M_{xy} \end{Bmatrix} = \int_{-h/2}^{h/2} \begin{Bmatrix} \sigma_x \\ \sigma_y \\ \tau_{xy} \end{Bmatrix} z \, dz \quad [2]$$

$$M_x = -D\left(\frac{\partial^2 w}{\partial x^2} + \nu \frac{\partial^2 w}{\partial y^2}\right) \quad [3a]$$

$$M_y = -D\left(\nu \frac{\partial^2 w}{\partial x^2} + \frac{\partial^2 w}{\partial y^2}\right) \quad [3b]$$

$$M_{xy} = -(1-\nu) D \frac{\partial^2 w}{\partial x \partial y} \quad [3c]$$

Here, D indicates the flexural rigidity of the plate which is equal to $D = \frac{Eh^3}{12(1-\nu^2)}$.

Now, the governing equation of the plate can be expressed as Equation 4:

$$\frac{\partial^2 M_{xx}}{\partial x^2} - 2\frac{\partial^2 M_{xy}}{\partial x \partial y} + \frac{\partial^2 M_{yy}}{\partial y^2} = N_x w_{xx} \quad [4]$$

The axial force N_x can be obtained with respect to the generalized strains as Equation 5

$$D(\nabla^4 w) = N_x \frac{\partial^2 w}{\partial x^2} \quad [5]$$

Where ∇^4 is commonly called the biharmonic operator.

As indicated above, the core material of the sandwich plate is considered with two constituents (i.e. ceramic and metal). Taking into account the Voigt homogenisation rule, the ceramic volume fraction V_c can be expressed as Equation 6 (Latifi et al., 2013; Baferani et al., 2011),

$$V_c(z) = \left(\frac{z}{h} + \frac{1}{2}\right)^k \quad [6]$$

And the volume fraction V_c and V_m satisfy Equation 7:

$$V_m(z) + V_c(z) = 1 \quad [7]$$

Where V_m is the corresponding volume fraction of metal, h is the plate cross-section height, and k is a gradient index in which $k \in [0, \infty)$, organises plate flexibility behaviour. By employing Equations 6 and 7, the effective mechanical properties of FGMs across the thickness of plate, considering the distribution of constituents follow a power-law is given by Equations 8 and 9:

$$\varphi(z) = \varphi_c V_c + \varphi_m V_m \quad [8]$$

$$\varphi(z) = \varphi_m + (\varphi_c - \varphi_m)\left(\frac{z}{h} + \frac{1}{2}\right)^k \quad [9]$$

Here φ_c and φ_m denote to effective properties of the FG plate materials (i.e. ceramic and metal), respectively (Merdaci et al. 2019; Singh & Harsha, 2020).

Mathematical Model for Porous FGM Sandwich Plate

For FG sandwich plate with even distribution of porosities (β <1) are considered to vary continuously within the thickness of the plate, expressions for, the elasticity modulus *E* and mass density of the imperfect FG core using the power-law distribution are described by Equations 10 and 11, while Poisson's ratio *v* is assumed not varies through-thickness direction (Nuttawit & Arisara, 2015; Kumar et al., 2021).

$$E(z) = E_m + (E_c - E_m)\left(\frac{z}{h} + \frac{1}{2}\right)^k - (E_c + E_m)\frac{\beta}{2} \quad [10]$$

$$\rho(z) = \rho_m + (\rho_c - \rho_m)\left(\frac{z}{h} + \frac{1}{2}\right)^k - (\rho_c + \rho_m)\frac{\beta}{2} \quad [11]$$

A rectangular sandwich plate assessed the linear buckling behaviour of an FGPM structure with total height *H* made of (Al/Al_2O_3) FG core with porous and two same isotropic face sheets is considered. As a result, the mechanical properties of upper and lower skins are the same (i.e. $E_1=E_2=E_f$ and $v_1= v_2= v$), and the thickness of both parts is the same (i.e., $h_1=h_2$), the corresponding flexural rigidity D_s can be represented in the following Equations 12, 13 and 14:

$$\begin{aligned} D_s &= \int_{-\left(\frac{h+h_1}{2}\right)}^{-\left(\frac{h}{2}\right)} \left\{\frac{z^2}{(1-v^2)}E(z)\right\} dz \\ &+ \frac{1}{(1-v^2)}\left(\int_{-\left(\frac{h}{2}\right)}^{\left(\frac{h}{2}\right)} \left\{E_m + (E_c - E_m)\left(\frac{z}{h} + \frac{1}{2}\right)^k \right.\right. \\ &\left.\left. - (E_c + E_m)\frac{\beta}{2}\right\} z^2 \right) dz + \int_{\left(\frac{h}{2}\right)}^{\left(\frac{h+h_2}{2}\right)} \left\{\frac{z^2}{(1-v^2)}E(z)\right\} dz \end{aligned} \quad [12]$$

$$D_s = \left(\frac{(E_c - E_m)h^3}{(1-v^2)} \left\{ \frac{1}{k+3} - \frac{1}{k+2} + \frac{1}{4(k+1)} \right\} + \frac{E_m h^3}{12(1-v^2)} - \frac{(E_c + E_m)\beta h^3}{24(1-v^2)} + \frac{E_f}{12(1-v^2)} \{(h+2h_1)^3 - h^3\} \right) \quad [13]$$

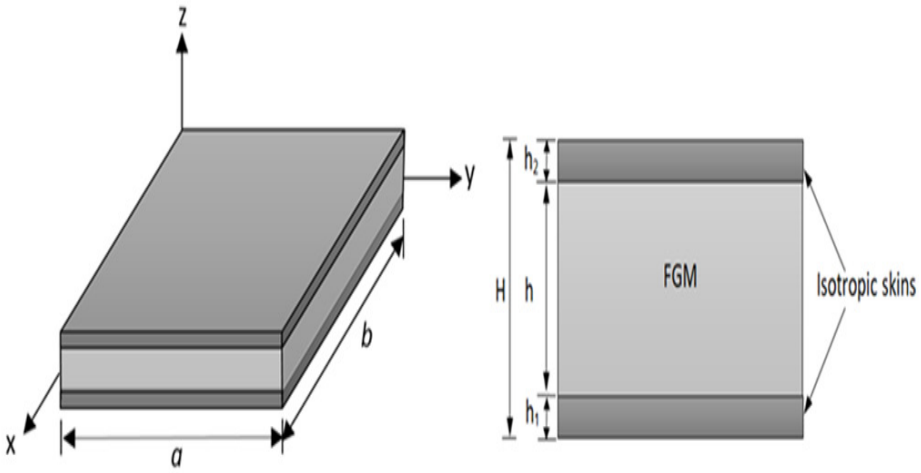

Figure 1. FGM Sandwich plate with porous core and homogenous skins

$$D_s \left(\frac{\partial^4 w}{\partial x^4} + 2\frac{\partial^4 w}{\partial x^2 \cdot \partial y^2} + \frac{\partial^4 w}{\partial y^4} \right) = N_x \frac{\partial^2 w}{\partial x^2} \quad [14]$$

and we may represent Equation 14 as follows (Equation 15):

$$\left\{ \frac{(E_c - E_m)h^3}{(1-v^2)} \left\{ \frac{1}{k+3} - \frac{1}{k+2} + \frac{1}{4(k+1)} \right\} + \frac{E_m h^3}{12(1-v^2)} - \frac{(E_c + E_m)\beta h^3}{24(1-v^2)} + \frac{E_f}{12(1-v^2)} \{(h+2h_1)^3 - h^3\} \right\} \times \left(\frac{\partial^4 w}{\partial x^4} + 2\frac{\partial^4 w}{\partial x^2 \cdot \partial y^2} + \frac{\partial^4 w}{\partial y^4} \right) = N_x \frac{\partial^2 w}{\partial x^2} \quad [15]$$

Here, and as an approximate solution, the function may be used to describe the behaviour of rectangular plate in x and y directions, and the stability Equation 15 may be written as Equation 16 (Al-Waily et al., 2020)

$$w = A_{mn} \sin \frac{m\pi x}{a} \sin \frac{n\pi y}{b} \quad [16]$$

where: *m*, *n* natural numbers (m, n=1, 2, 3, . . .), also, A_{mn} is a constant coefficient, then by substituting the supported boundary conditions, into Equation 16, and putting through Equation 15,
we get Equations 17 and 18,

$$N_x = \left\{ D_s \times \left(\frac{m\pi}{a}\right)^2 + 2D_s \times \left(\frac{n\pi}{b}\right)^2 + D_s \times \left(\frac{n\pi}{b}\right)^4 \left(\frac{a}{m\pi}\right)^2 \right\} \quad [17]$$

$$N_x = \left\{ D_s \times \left(\frac{\pi}{a}\right)^2 + 2D_s \times \left(\frac{\pi}{b}\right)^2 + D_s \times \left(\frac{\pi}{b}\right)^4 \left(\frac{a}{\pi}\right)^2 \right\} \quad [18]$$

Consequently, the stability of an imperfect sandwich plate can be evaluated by determining the critical value of buckling load N_x. Moreover, in the case of the fundamental critical buckling occurs ($m = n = 1$), one may directly arrange Equation 18 for the square sandwich plate, which leads to getting Equation 19:

$$N_x = 4D_s \left(\frac{\pi}{a}\right)^2 \quad [19]$$

Using MATLAB code, the critical buckling load of Equation 17 may be determined, and different results can be recorded.
In consequence, the critical stress takes the following form as Equation 20,

$$\sigma_{x,cr} = \frac{N_{x,cr}}{h} \quad [20]$$

Furthermore, the associated dimensionless of the critical buckling load of thin porous FGM sandwich plates $\overline{N}$ can be written as Equation 21:

$$\overline{N} = N_{x,cr} \frac{a^2}{E_m h^3} \quad [21]$$

Experimental Work

The experimental program covers the design of the specimens used as well as compression tests utilising samples with three porosity values (β = 0.1, 0.2, and 0.3), a gradient index (k=1), and skins with a thickness of 1 mm using (Tinius Olsen H50KT) apparatus. In addition, a computer-controlled testing apparatus was used to measure maximum compression load and maximum total deflection at the mid-span of the plates.

Design and Preparation of the FG Test Specimens

In this study, two additively manufactured (AM) materials, Polytropic acid (PLA) and Thermoplastic polyurethane (TPU), produced by FlashForge (Zhejiang Hisun Biomaterials,

China), were used for 3D printing with a standard diameter of 1.75 mm. Each type has unique properties and applications that distinguish them from one another. All the samples were designed with porosity using Solid Works, then saved as a (.stl) file, then used to construct the sample with a CR-10 Max 3D printer. Throughout the current study, the face sheet was constructed mainly from aluminium alloy (AA6061-T6) plates with a thickness of 1 mm, the material most widely used for engineering applications and aerospace structures. On both top and bottom surfaces of the face sheet, extra adhesion (Epoxy) is used to bond it to the FG core, as shown in Figure 2. Table 1 summarises the mechanical properties of the FG core and face sheet (Arndt & Lechner, 2014; Balakrishna et al., 2020).

Figure 2. Manufacturing FG plate specimens using 3D printing

Table 1

Material properties of sandwich plates used in experimental work

Material	E (GPa)	ρ (Kg/m^3)	ν
PLA	1.2	1360	0.38
TPU	2.58	1450	0.35
AA6061-T6	70	2702	0.3

Experimental Setup and Procedure

Sandwich plates composed of functionally graded porous metals can be used for buckling experiments. The test specimens were fabricated from FGM with dimensions of 150 x 300 and 10 and 15 mm core heights. The plate is mounted on fixtures, and the experiment is conducted under (SFSF) boundary conditions. All experiments are carried out on

electromechanical universal testing equipment (UTM). The specimen was subsequently compressed unidirectionally at a displacement-controlled rate of 0.5 mm/min (in the direction of the y-axis). The force-extension curve drawn using UTM, as shown in Figure 3, can be used to establish the critical buckling load value for the plate structure under the impact of various parameters. The test technique was conducted three times on samples with the same attributes to ensure accuracy. Finally, the integral test method was repeated for all samples.

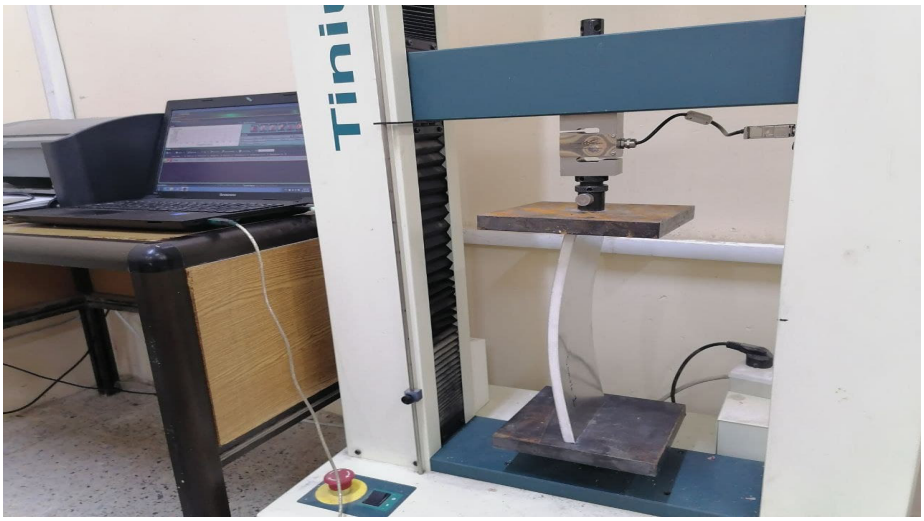

Figure 3. Experimental setup for FG sandwich plates

Numerical Investigation

The finite element method (FEM) is an excellent numerical way to analyse the dynamic response and the prediction of total deformation load, at which point stability can be observed in the FGMs sandwich plate (Emad et al., In Press; Vyacheslav & Tomasz, 2020). Accordingly, the numerical model of the sandwich plate with porous metal is carried out by employing the ANSYS software (Ver. 2021 R1). The 3D finite element model with dimensions a=b=0.5 m. The FG parameters include porosity coefficients Beta (0-0.3), the thickness of the core varies from (5-25) mm, and the gradient index k is (0-5). The skin thickness is kept to be 2.5 mm for upper and lower surfaces. For the mesh refinement process to work well, further mesh refining and convergence approach was carried out to get high accuracy numerical results, as shown in Figure 4, which uses 2536100 nodes. In the simulation, the material properties used in linear buckling analysis are calculated after mathematical operations, then involved as a new assignment into the model engineering data view. The desired model requires a thin layer of glue to pass through the connection area and between the layers to attain accurate results.

Furthermore, the glue prevents uneven thickness development between layers and skins caused by inconsistent settlement (Nguyen et al., 2020). In addition to the characteristics of the plate, the system also includes the mechanical characteristics of top and bottom skins. As such, apply the corresponding BC's under uniaxial compression on both plate sides. The square FG sandwich plate with supported boundary conditions subjected to uniaxial load case is illustrated in Figure 5. Next, buckling analysis of the selected models may be obtained to discover the stability behaviour in terms of total deformation load.

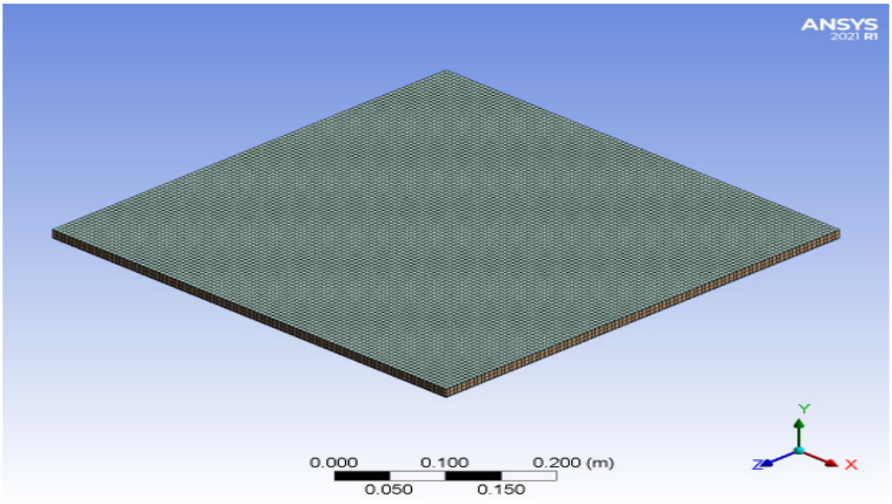

Figure 4. The model of FG system with Mesh

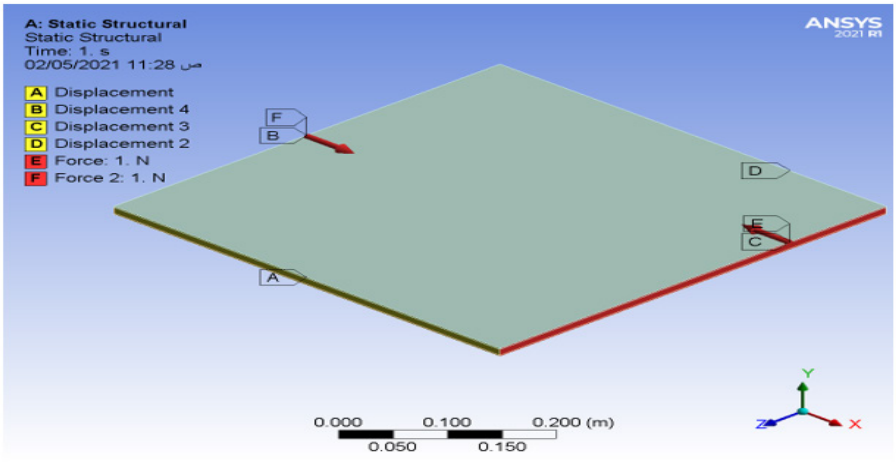

Figure 5. FGM Sandwich plate with S.S boundary conditions

Optimisation Problem Formulation

Topology optimisation can provide an optimised design and a better approximation based on a series of loads and constraints. Furthermore, by considering the buckling limit to minimise structural compliance, the buckling limit may determine an acceptable level of withstanding to total deformation of the structure (Mrinal & Manish, 2021; Sadiq et al., 2021; Lin et al., 2019). This work's scope optimisation includes a detailed design of a porous FG structure with specified boundary conditions under the influence of linear buckling using ANSYS 2021 R1, as shown in Figure 6. By including RSM, the model is built, meshed, and the design parameters are introduced, and the response results for total deformation, buckling load, and equivalent stresses are obtained.

Based on the fact that FG parameters have a considerable impact on handling the FGM sandwich structure stability problem, the design of experiment software (DOE) was employed: to study the influence of the FG parameters on stability, obtaining optimal parameters, and develop a mathematical model based on numerical data. The well-known optimisation procedure known as the MOGA method is used. It provides frequent purposes and constraints to determine the optimum global concept. The design variables involving skin thicknesses (*P1*), core height (*P3*), porous parameters (*P8*), and power-law index (*P9*) are selected with appropriate limits, as it is found in Table 2. The main objective of this study is the maximise Total Deformation Load Multiplier (P15), Total Deformation Maximum (mm) (P18), Equivalent Stress Maximum (MPa) (P19), and Force Magnitude 1and 2 (N) (P16 & P17), respectively considering initial samples 4000 and the number of samples per iteration 800 with a maximum of 13 iterations for each process. Moreover, the number of candidates is 3. The most important convergence roles in optimisation work involve Pareto and stability criterion. The estimated number of evaluations is 19200. Numerical simulation cases were conducted based on the design matrix established by the design of experiment (DOE) software.

In particular, to get many results, special software known as dxrom combines with ANSYS DesignXplorer Add-in for Excel. One may select any variable of the input parameters, apply any sampling point from (1 to 100), and select X and Y values. We can generate frequent results represented by tables and plots through this scope. Furthermore, we can choose any response point and performed the same work. Also, the percentage error can be obtained for each solution.

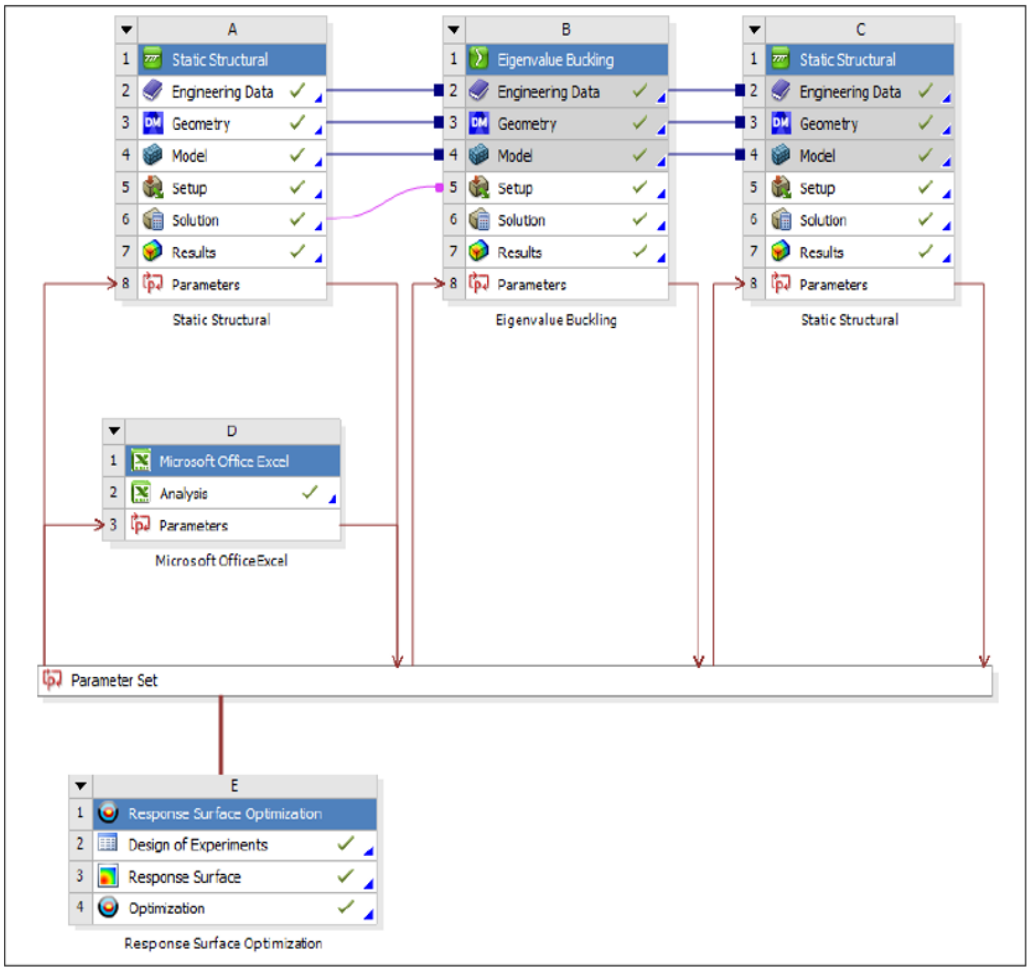

Figure 6. View of optimisation analysis via Ansys

Table 2

Limits of design parameters

Parameter	Symbol	Minimum value	Maximum value
Skin thickness (m)	(*P1 / a1*)	0.002	0.0025
Plate thickness (m)	(*P3 / b1*)	0.005	0.025
Porosity coefficient	(*P8 / Beta*)	0	0.5
Volume fraction index	(*P9 / K*)	0	5

RESULTS AND DISCUSSION

This paper presents buckling analysis and the stability problem of FGPMs. The FGM core layers are considered to be graded via the thickness direction of the plate with an even arrangement of porosities. A new mathematical formulation is carried out based on CPT, and the second-order differential equation is derived and solved. Many important parameters are tested to check their effects on the critical buckling load. These parameters include porosity ratio, gradient index, number of FGM platelayers, and aspect ratio. The analytical solution is validated by conduct a numerical investigation using the ANSYS 2021 R1. Various results are introduced and organised in multiple tables and figures. The mechanical properties for the FGM core, made from a mixture of (Al_2O_3/Al) and mild steel skins, are given in Table 3 (Cui et al., 2019). The plates have identical length and width (a=b=0.5m), the porosity ratio β (0 to 50%), the power-law distribution k (0 to 5), the FG core height h (5 to 25)mm, and two values of the skin thickness h_1 (2 and 2.5) mm.

Table 3

Material properties of the FG sandwich plate used in numerical and analytical solutions

Property	FG core		Face Sheets (Steel)
	Aluminium (Al)	Ceramic (Al_2O_3)	
E (GPa)	70	380	210
ρ (Kg/m^3)	2700	3800	7800
ν	0.30	0.30	0.30

The nondimensional of critical buckling load is given as Equation 22:

$$\overline{N} = N_{x,cr}(a^2/E_m h^3) \quad [22]$$

The proposed analytical solution capability for evaluating the linear buckling load of the functionally graded sandwich plate with porosity is examined. The dimensionless buckling load of the imperfect square sandwich plate is determined and compared with those calculated by FEA and introduced in Table 4. The dimensions of the plate are a=b= 0.5 m, and the (Al/Al_2O_3) constituents FG core height (h = 10 mm). Meanwhile various porosity factors *Beta* (i.e., *Beta* = 0.1,0.2,0.3, 0.4 and 0.5) are considered and the power-law index k=1. The results were in good convergence with an average percentage error of 5%. One may discover that all models were utilising the critical value of buckling load induced in FG sandwich plate decrease with the increase of both power-law exponent and porosity parameters due to a clear decrease in material stiffness. Table 5 demonstrates the variation

of critical buckling loads of SFSF sandwich plate composed of PLA (Polytropic acid) and TPU (Thermoplastic Polyurethane) porous metal. The results show a good agreement between the UTM results and those obtained by the simulation procedure, with a maximum error percentage of 12% occurring at slenderness ratio $a/H = 30$ and porosity factor = 0.3. Furthermore, from the results, it may be concluded that TPU is an elastic polymer. Hence it may be used in various applications, such as car instrument panels and medical devices.

Table 4

Buckling load parameter results obtained by analytical and numerical solutions of supported Al/Al_2O_3 FGPMs sandwich plate(a/b=1)

No.	h_1	h	β	k	Buckling load parameter		Discrepancy %
					Analytical	Numerical	
1	2.5	10	0.0	0.5	11.347	11.75	3.429
2	2.5	10	0.1	0.5	11.104	11.476	3.241
3	2.5	10	0.2	0.5	10.65	10.95	2.739
4	2.5	10	0.3	0.5	10.317	10.624	2.889
5	2.5	10	0.4	0.5	10.174	10.365	1.842
6	2.5	10	0.5	0.5	9.931	9.995	0.640

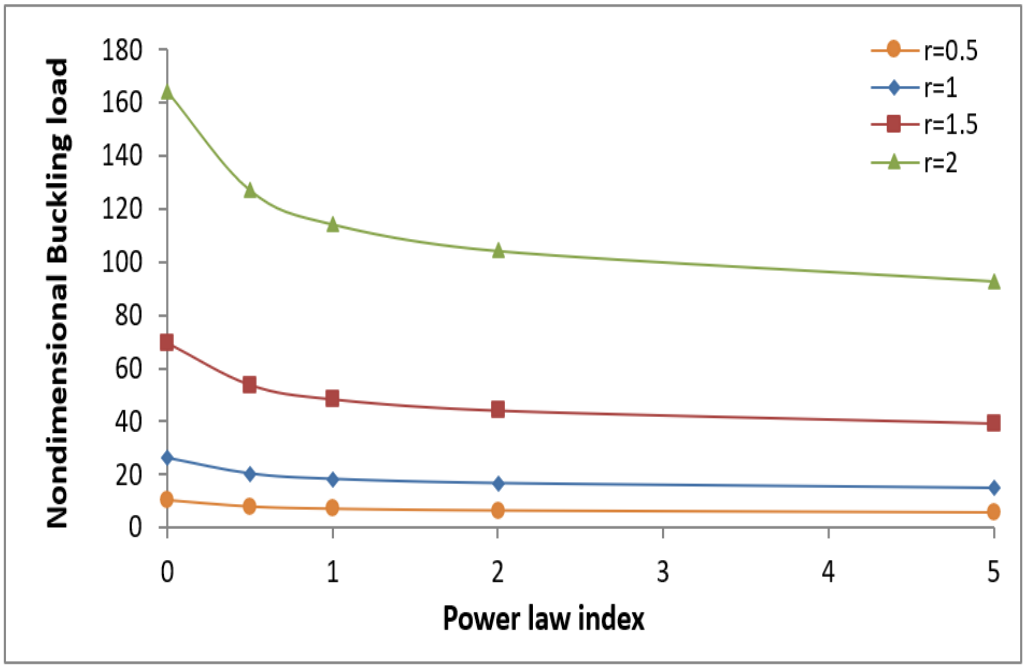

Figure 7. Convergence of the buckling load parameter results of supported (Al/Al_2O_3) FGPMs sandwich plates for different slenderness ratios.

Figure 7 shows the buckling load parameters results obtained by the proposed analytical solution of the supported porous FGM sandwich plate involving aspect ratio impact for five different values (r=0.5,1,1.5, and 2) at porous factor (β=0.1), and the ratio of core to skin thickness (h/h_1=5). It can be seen from Figure 7 that as the volume fraction and aspect ratio gradually increase, ($\bar{N}$) increases, and the influence of the gradient index k is more significant as the aspect ratio increases (i.e. the effect of power-law exponent disappears at small values of aspect ratios). According to the details of Figure 8, the analytical solution results for the dimensionless parameter ($\bar{N}$) are given at porosity parameter (β= 0,0.1,0.3), for the various core to skin thickness ratio (h/h_1 =2,4,6,8,10) at gradient index (k=0.5). It is observed that the critical buckling loads parameter is decreased with the increase of both cores to face-sheet thickness ratio (h/h_1) and porosity coefficient (β). Also, there is a clear convergence in results with an increased thickness ratio from 6 to 10. One may be concluded that the bending stiffness of the sandwich plate is significantly affected with the increase of core to face-sheet thickness ratio h/h_1 due to a decrease in overall stiffness. By considering the FGM sandwich plate comprised of layers up to 20, Figure 9 presents the buckling load parameter results due to the Ansys simulation at porosity coefficient (β=0.25). The results obtained for different aspect ratios including value of power-law index (k= 1), core height (h=10 mm), and face sheet thickness (h_1 = 1.5mm). It is found that there are no obvious variations of buckling load parameters when the structure core is constructed by a few layers as well as a small aspect ratio. However, the performance of the whole structure offers high stability as the number of FG core layers increases.

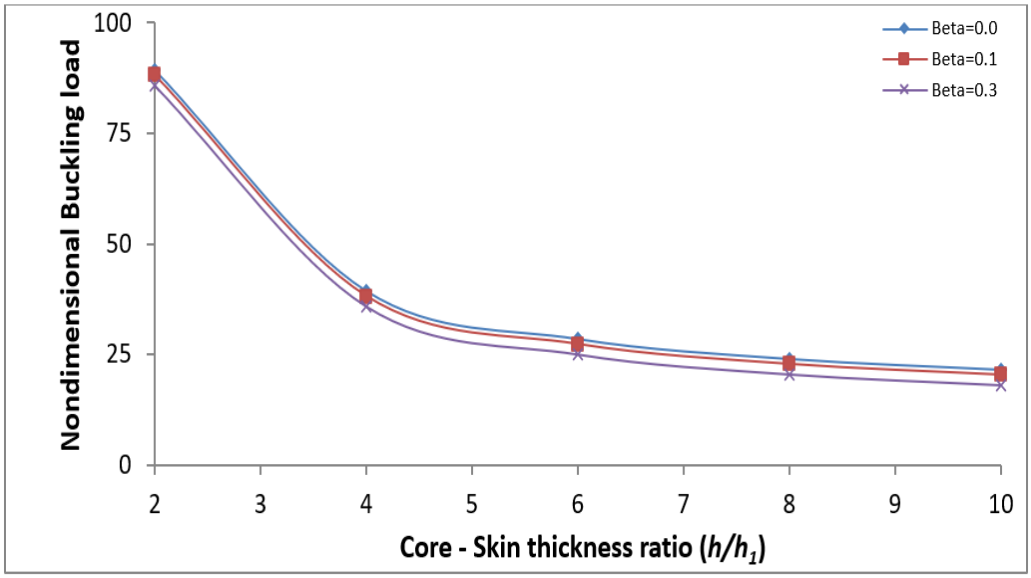

Figure 8. A comparison of the critical buckling load parameter of a square sandwich plate having three porosities, h/h_1, in terms of the core to face-sheet thickness ratio.

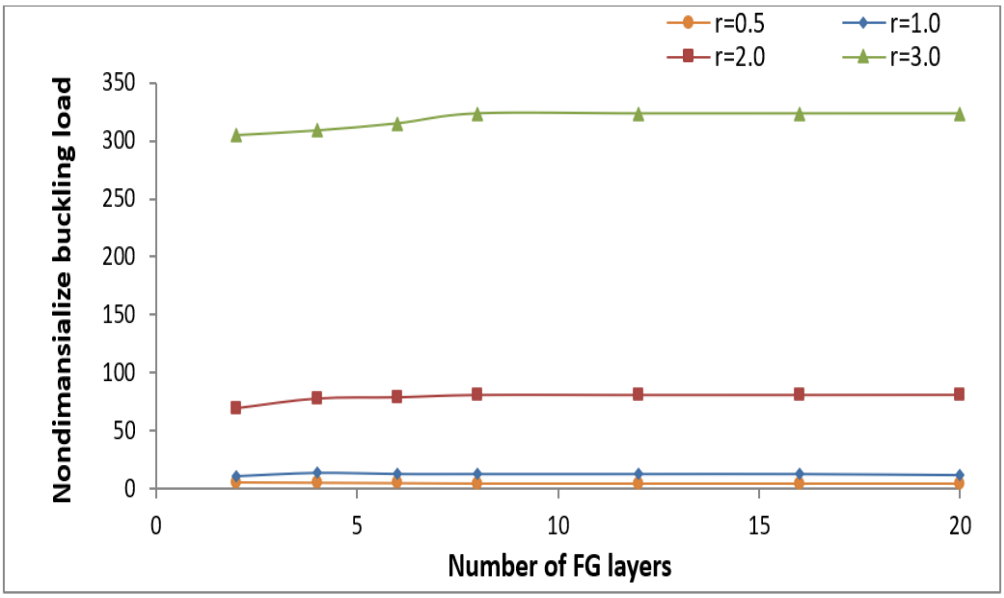

Figure 9. Results of the $\overline{N}$ of rectangular FGM sandwich plate, for various aspect ratios at k=1

Table 5

Experimental and numerical variation of critical buckling loads of SFSF rectangular sandwich plate, skin thickness 1mm

Sandwish type	*b/a*	*a/H*	Porosity	Experimental (N)	Numerical (N)	Discrepancy %
PLA/Al	0.5	30	0	11750	12984.924	9.51
			0.1	11480	12362.883	7.14
			0.2	11179	11870.840	5.83
			0.3	10750	11618.802	7.48
	0.5	20	0	32100	33514.204	4.23
			0.1	31550	33396.080	5.53
			0.2	31000	33277.955	6.85
			0.3	30645	33159.831	7.58
TPU/Al	0.5	30	0	11200	11665.2	3.98
			0.1	10890	11635.38	6.41
			0.2	10455	11621.87	10.04
			0.3	10180	11568.37	12.00
	0.5	20	0	27175	28165.52	3.52
			0.1	26490	27982.29	5.33
			0.2	26750	27924.33	4.21
			0.3	26110	27866.37	6.30

Table 6 also shows Ansys's critical buckling load parameter results for sandwich plates employing different porosity coefficients under five types of boundary conditions. For example, the plate thickness ratio $a/h = 50$, and thickness of face sheets 2mm. Influences of porosity coefficient and power-law index are investigated, and it is noticed that the higher buckling parameter value present at the model stronger constraints. As an example, taking into accounts the porosity coefficient ($\beta = 0.1$) and the gradient index ($k = 1$), The buckling parameter for the CCCC model is 17, while in CCCS, the buckling parameter is 15.75, also in CCCF, the buckling parameter is 13.79, as for SCSC, the buckling parameter is 12.79, and in SSSS, the value is 10.73. It is concluded that the critical buckling load increases with the increase in the constraints to the boundary conditions; for example, the frequency parameter for CCCC is higher than CCCS, and this condition is more than CSCS, and so on.

Table 6

Results of FEA solution of $\overline{N}$*, with different boundary conditions at thickness ratio (a/h =100)*

B.C.'s	k	Porosity factor					
		0	0.1	0.2	0.3	0.4	0.5
CCCC	0	18.99	18.68	17.99	17.66	17.32	17.17
	0.5	17.87	17.67	17.46	17.13	16.99	16.69
	1	17.54	17.11	16.85	16.79	16.55	16.43
	2	17.11	16.78	16.52	16.38	16.10	15.99
	5	16.59	16.45	16.21	15.99	15.88	15.71
CCCF	0	14.85	14.65	14.42	14.21	14.09	13.93
	0.5	14.31	14.27	14.06	13.92	13.85	13.70
	1	14.01	13.95	13.72	13.61	13.50	13.12
	2	13.75	13.66	13.41	13.38	13.09	12.94
	5	13.50	13.22	13.15	12.95	12.74	12.42
SCSC	0	13.88	13.50	13.26	13.01	12.85	12.54
	0.5	13.35	13.12	12.97	12.71	12.49	12.11
	1	13.00	12.79	12.45	12.20	12.01	11.60
	2	12.50	12.20	12.07	11.87	11.40	11.20
	5	11.86	11.51	11.31	11.19	11.06	10.87
SSSS	0	12.34	12.13	11.94	11.71	11.53	11.32
	0.5	11.27	11.11	10.88	10.68	10.48	10.31
	1	10.97	10.73	10.53	10.35	10.16	9.920
	2	10.64	10.48	10.28	10.10	9.89	9.650
	5	10.37	10.16	9.967	9.750	9.58	9.380

Table 6 *(Continued)*

B.C.'s	k	Porosity factor					
		0	0.1	0.2	0.3	0.4	0.5
CCCS	0	16.84	16.59	16.26	16.09	15.87	15.71
	0.5	16.32	16.02	15.99	15.70	15.61	15.48
	1	15.81	15.75	15.61	15.55	15.31	15.00
	2	15.61	15.34	15.18	15.01	14.82	14.60
	5	15.09	14.88	14.79	14.58	14.37	14.12

Response Surface Results

Response surface methodology is another common statistical approach for process parameter optimisation. It includes 3D figures to display how certain input design values will impact the response view of resultant parameters. Figure 10 represents the total deformation buckling load response chart at gradient index $k = 0$, while Figure 11shows the maximum equivalent stress with varying porosity parameters and core height at gradient index k=0.5. From Figures 10 and 11, it is found that both buckling load and equivalent stress increase with the decrease of gradient index and porosity coefficients. Furthermore, a response chart for both equivalent stresses and deformation load is shown in Figures 12 and 13. In terms of the porosity parameter, it is demonstrated that the presence of pores influences the overall rigidity of functionally graded structures. We can also generate graphs of Local Sensitivity to display relationships of each input parameter with corresponding output parameters. Simultaneously by constructing a spider chart, changing the input parameters may visualise the effect on all the output parameters.

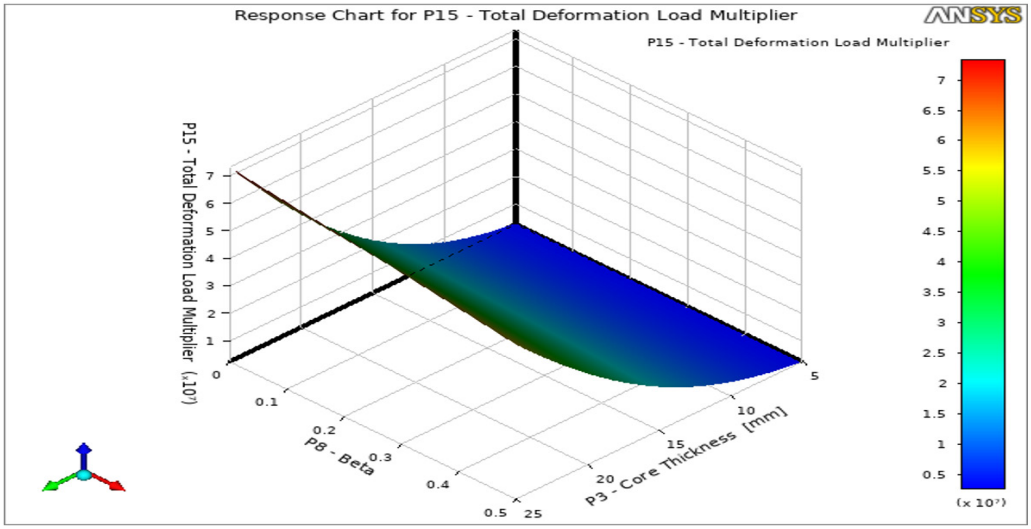

Figure 10. RSM with varying parameters for total deformation multiplier at k=0

Table 7

Optimisation results for three candidate points for total deformation load

Candidate points	P_1 (mm)	*P3* (mm)	P8	P9	Total Deformation Load Multiplier
1	2.5	20	0.3	3	353636
2	2.5	19.857	0.299	2.999	677775
3	2.5	19.678	0.299	3	785788

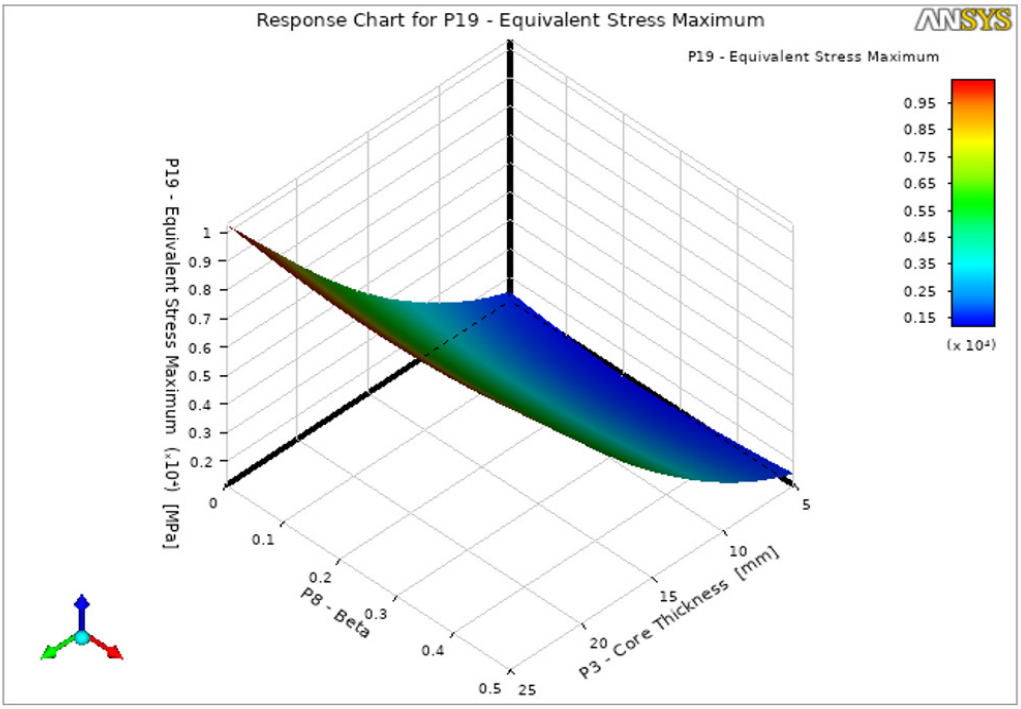

Figure 11. RSM with varying parameters for equivalent stresses at k =0.5

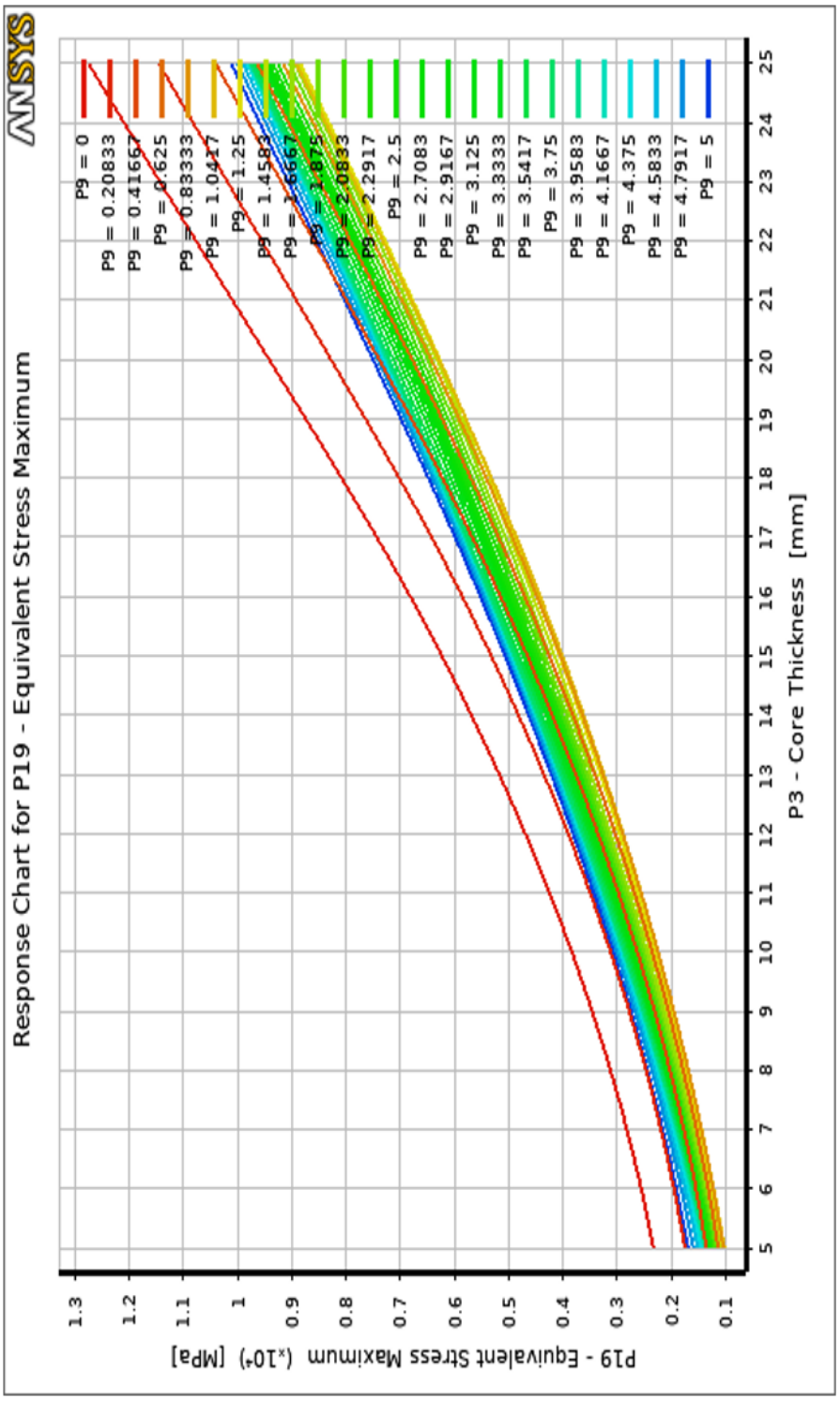

Figure 12. Response chart for Equivalent Stresses

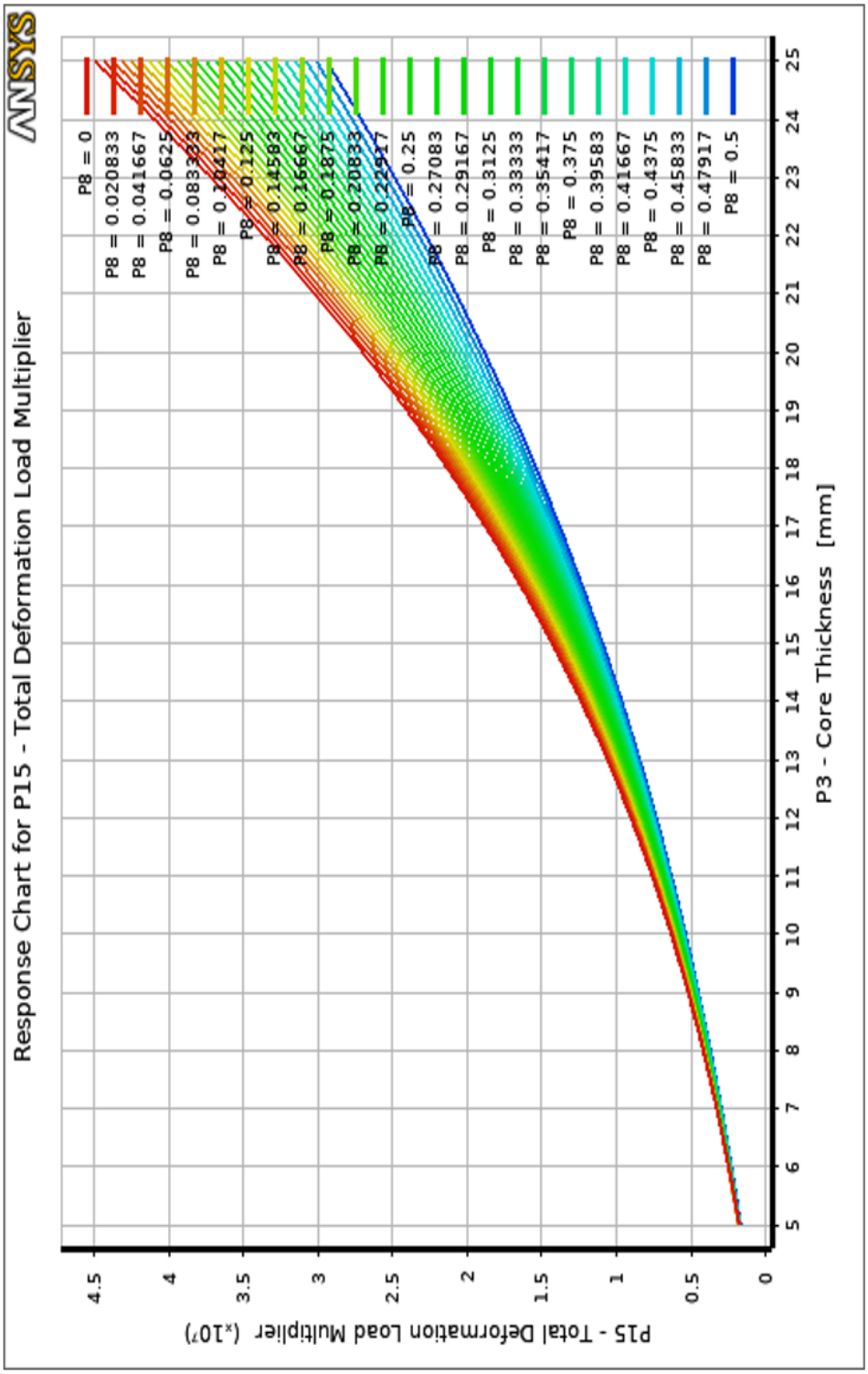

Figure 13. Response chart for Total Deformation Load

Optimisation Results and Discussion

This section deals with frequent results obtained by optimisation work. It is included but is not limited to the Tradeoff charts, Sensitivities, and Candidate points. Table 7 presents three candidate points results found by optimisation work. The results indicated that a generated design for all models has an excellent tendency to predict the stability of porous FG sandwich structures. Specifically, feasible points for total deformation load and equivalent stresses are introduced in the Tradeoff charts as shown in Figures 14 and 15, respectively. According to details in Figures 15 and 16, it is found that the gradient index k = 0 results in a sharp gradient in both total deformation and equivalent stress near the bottom surface of the plate, while k = 2.9 results in a steep gradient in total deformation equivalent stress near the top surface. The reason for this is the sharply varying material properties near the top and bottom surfaces for k = 0 and 3.

Figure 16 presents a graphical view of the global sensitivities for total deformation load multiplier, equivalent stresses, and force magnitude with respect to the input parameters such as skin, core heights, porosity coefficient, and FG constituent index. Sensitivity with positive response occurs when an apparent increase of the input parameter yields to an increase in output response. In contrast, a negative sensitivity can be seen when an inverse relationship between input and output occurs.

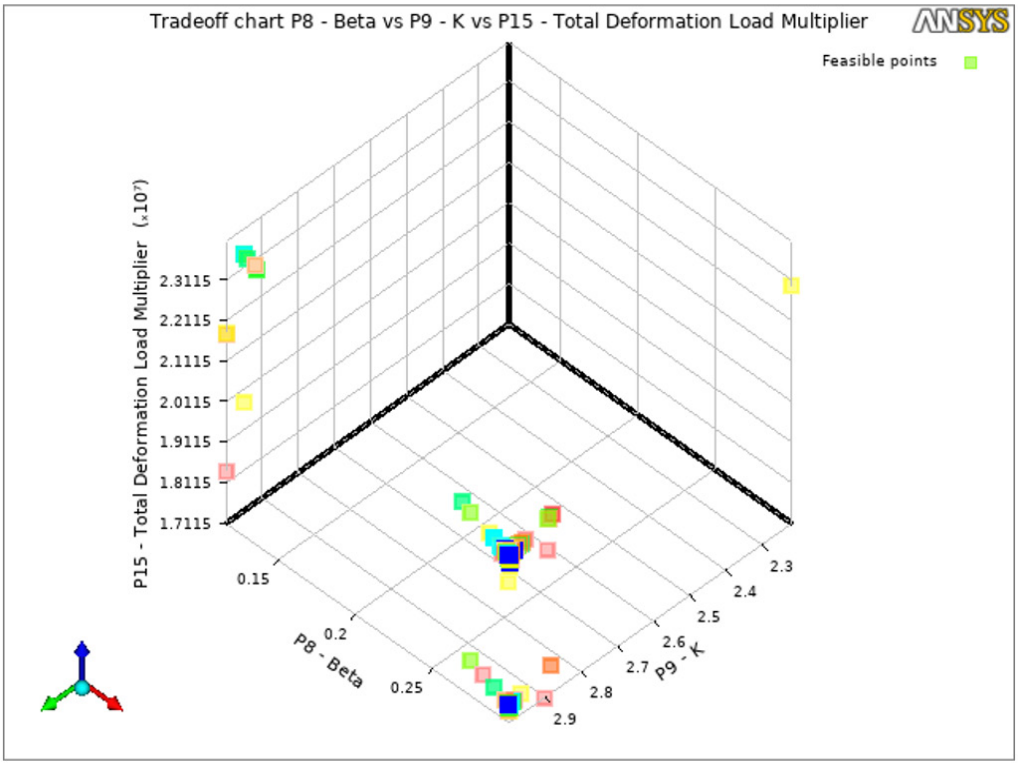

Figure 14. Tradeoff chart for Total deformation load at a number of Pareto to show 8 feasible points

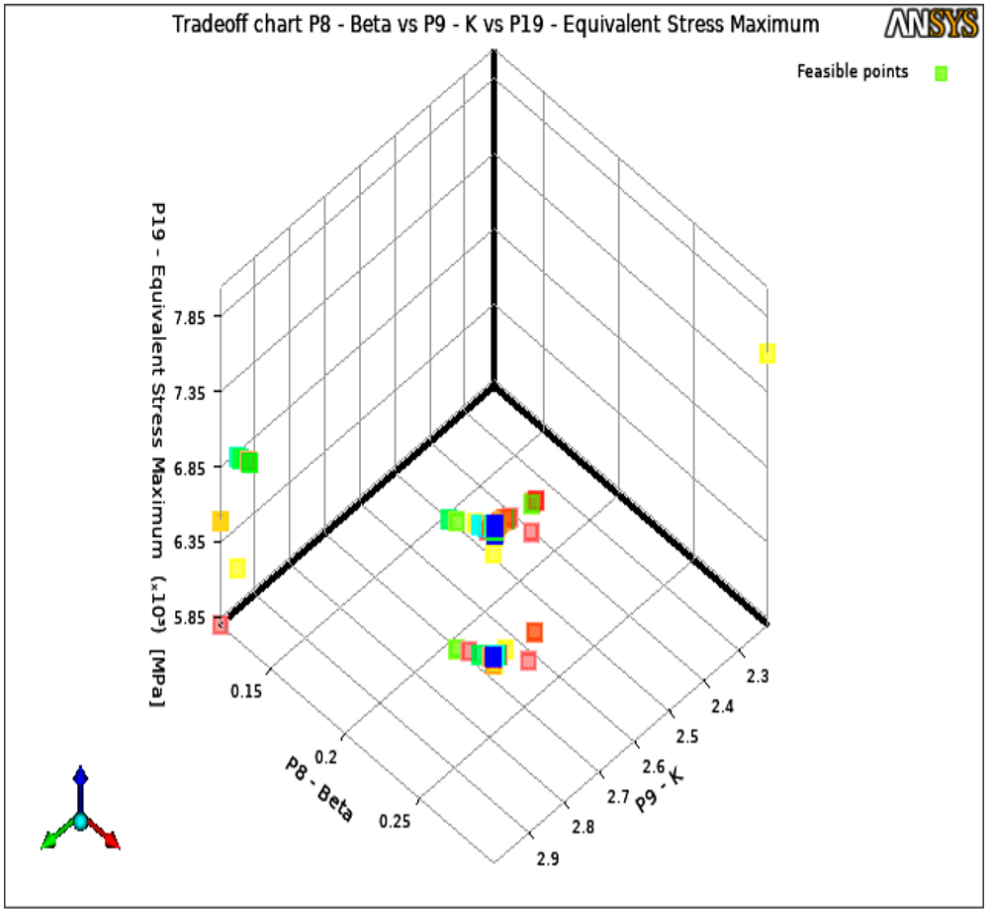

Figure 15. Tradeoff chart for Equivalent stress at a number of Pareto to show 8 feasible points

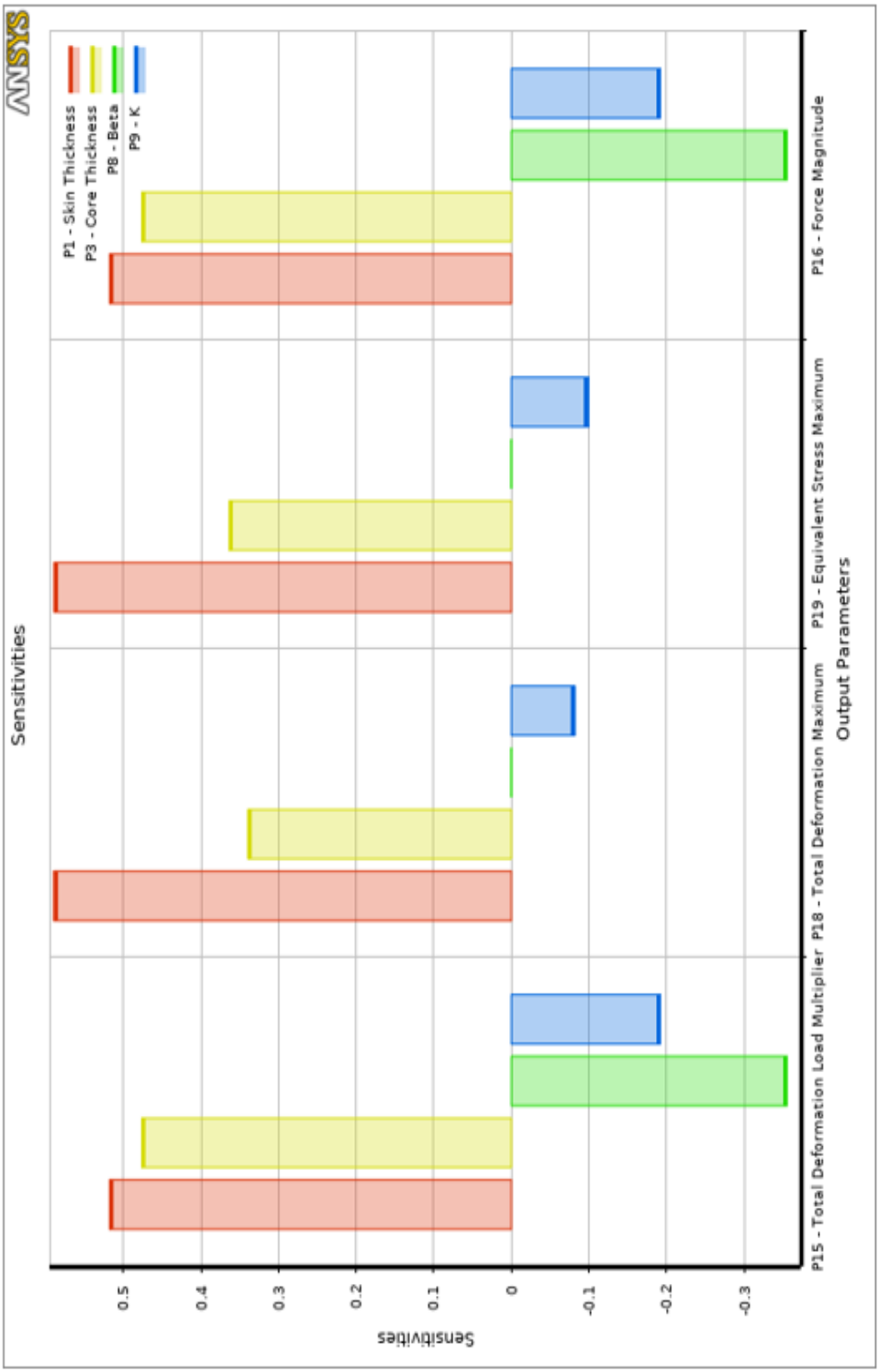

Figure 16. Sensitivities for various parameters

CONCLUSION

Porous FG materials are widely used in many applications such as tissue engineering, Biomedicine, and aerospace. The present work investigates the MOGA optimisation method for eigenvalue buckling analysis of supported functionally graded sandwich plate with Al/Al_2O_3 porous core and two homogeneous material skins. The presented generalised analytical model employing the classical plate theory of the sandwich structure is formulated. The FEA approach confirmed the correctness of the generalised analytical model of the sandwich structure with FGMs. Results for important parameters of FG core material and thickness and type of boundary conditions are evaluated. Some concluding observations from the investigation are given below.

- For all the boundary conditions, the buckling load increases with an increased aspect both thickness *a/h*) and slenderness ratio (*a/b*).
- It can be observed that the performance of sandwich structures with porous FG is influenced by, type of the axial load, volume fraction characteristics, and boundary conditions. Also, it was found that the maximum critical buckling load of such a sandwich plate is gained when, pure ceramic surface, its supports are completely clamped, and the porosity factor is 0.1.
- The FEA models represented by Ansys software are a high-quality way to design, optimize, and predict critical buckling load. Hence it can identify the stability and level of performance of the FGM sandwich structure.
- A reasonable agreement was established between the experimental and finite element analysis using ANSYS software for buckling analysis, with a percentage error of no more than 15%, indicating that there was no delamination between the layers of FGM samples and that the test samples were well-fabricated.
- The behaviour of the sandwich structure is positively influenced by the ratio of core height to total sandwich plate height (i.e. *h/H*). It is because the rigidity of the sandwich panel is greatly affected by this ratio.
- According to the results obtained by the DOE and RSM, the resulted optimum value for the maximum porosity coefficient was found at 0.3, core height (0.019678 m), face sheet thickness (0.0025 m), and the maximum gradient index (3), where the optimum total deformation load multiplier value was found (785788).

ACKNOWLEDGEMENT

The authors appreciate the cooperation of the University of Kufa and the University of Technology/Iraq in completing the experimental work.

REFERENCES

Abo-bakr, R. M., Abo-bakr, H. M., Mohamed, S. A., & Eltaher, M. A. (2021). Optimal weight for buckling of FG beam under variable axial load using Pareto optimality. *Composite Structures, 258*, Article 113193. https://doi.org/10.1016/j.compstruct.2020.113193

Al-Waily, M., Al-Shammari, M. A., & Jweeg, M. J. (2020). An analytical investigation of thermal buckling behavior of composite plates reinforced by carbon nano-particles. *Engineering Journal, 24*(3), 11-21. https://doi.org/10.4186/ej.2020.24.3.11

Arefi, M., & Najafitabar, F. (2021). Buckling and free vibration analyses of a sandwich beam made of a soft core with FG-GNPs reinforced composite face-sheets using Ritz Method. *Thin-Walled Structures*, *158*, Article 107200. https://doi.org/10.1016/j.tws.2020.107200

Arndt, K. F., & Lechner, M. D. (2014). *Polymer solids and polymer melts–mechanical and thermomechanical properties of polymers*. Springer. https://doi.org/10.1007/978-3-642-55166-6

Baferani, H. A., Saidi, A. R., & Ehteshami, H. (2011). Accurate solution for free vibration analysis of functionally graded thick rectangular plates resting on elastic foundation. *Composite Structures, 93*(7), 1842-1853. https://doi.org/10.1016/j.compstruct.2011.01.020

Bai, L., Yi, C., Chen, X., Sun, Y., & Zhang, J. (2019). Effective design of the graded strut of BCC lattice structure for improving mechanical properties. *Materials, 12*(13), Article 2192. https://doi.org/10.3390/ma12132192

Balakrishna, A., Padmanav, D., & Singh, N. B., (2020). Buckling analysis of porous FGM sandwich plates under various types nonuniform edge compression based on higher order shear deformation theory. *Composite Structures, 251*, Article 112597. https://doi.org/10.1016/j.compstruct.2020.112597

Bassiouny, S., Jinghua, J., Reham, F., Tareq, A., Qiong, X., Lisha, W., Dan, S., & Aibin, M. (2020). 30 years of functionally graded materials: An overview of manufacturing methods, applications, and future challenges. *Composites Part B: Engineering, 201*, Article 108376. https://doi.org/10.1016/j.compositesb.2020.108376

Chen, D., Yang, J., & Kitipornchai, S. (2019). Buckling and bending analyses of a novel functionally graded porous plate using Chebyshev-Ritz method. *Archives of Civil and Mechanical Engineering*, *19*(1), 157-170. https://doi.org/10.1016/j.acme.2018.09.004

Chen, Z., Li, J., Sun, L., & Li, L. (2019). Flexural buckling of sandwich beams with thermal-induced non-uniform sectional properties. *Journal of Building Engineering, 25*, Article 100782. https://doi.org/10.1016/j.jobe.2019.100782

Cui, J., Zhou, T., Ye, R., Gaidai, O., Li, Z., & Tao, S. (2019). Three-dimensional vibration analysis of a functionally graded sandwich rectangular plate resting on an elastic foundation using a semi-analytical method. *Materials, 12*(20), Article 3401. https://doi.org/10.3390/ma12203401

Emad, K. N., Al-Waily, M., & Sadeq, H. B. (In Press). Optimization design of vibration characterizations for functionally graded porous metal sandwich plate structure. *Materials Today: Proceedings*. https://doi.org/10.1016/j.matpr.2021.03.235

Emad, K. N., Al-Waily, M., & Sadeq, H. B. (2021a). A review of the recent research on the experimental tests of functionally graded sandwich panels. *Journal of Mechanical Engineering Research and Developments, 44*(3), 420-441.

Emad, K. N., Al-Waily, M., & Sadeq, H., B. (2021b). A critical review of recent research of free vibration and stability of functionally graded materials of sandwich plate. *IOP Conference Series: Materials Science and Engineering, 1094*, Article 012081. https://doi.org/10.1088/1757-899X/1094/1/012081

Hessameddin, Y., & Farid T. (2020). Analytical solution and statistical analysis of buckling capacity of sandwich plates with uniform and non-uniform porous core reinforced with graphene nanoplatelets. *Composite Structures, 252*, Article 112700. https://doi.org/10.1016/j.compstruct.2020.112700

Jin, X. S., & Masatoshi S. (2015). Interface shape optimization of designing functionally graded sandwich structures. *Composite Structures, 125*, 88-95. https://doi.org/10.1016/j.compstruct.2015.01.045

Krzysztof, M., & Ewa, M., (2021). Generalization of a sandwich structure model: Analytical studies of bending and buckling problems of rectangular plates. *Composite Structures, 255*, Article 112944. https://doi.org/10.1016/j.compstruct.2020.112944

Kumar, V., Singh, S. J., Saran, V. H., & Harsha, S. P. (2021). Vibration characteristics of porous FGM plate with variable thickness resting on Pasternak's foundation. *European Journal of Mechanics - A/Solids, 85*, Article 104124. https://doi.org/10.1016/j.euromechsol.2020.104124

Latifi, M., Farhatnia, F., & Kadkhodaei, M. (2013). Buckling analysis of rectangular functionally graded plates under various edge conditions using Fourier series expansion. *European Journal of Mechanics - A/Solids, 41*, 16-27. https://doi.org/10.1016/j.euromechsol.2013.01.008

Lin, C., Bai, J., & Albert, C. (2019). Functionally graded lattice structure topology optimization for the design of additive manufactured components with stress constraints. *Computer Methods in Applied Mechanics and Engineering, 344*, 334-359. https://doi.org/10.1016/j.cma.2018.10.010

Merdaci, S., Belmahi, S., Belghoul, H., & Hadj, M. A. (2019). Free vibration analysis of functionally graded plates FG with porosities. *International Journal of Engineering & Technical Research, 8*(3), 143-147. https://doi.org/10.17577/IJERTV8IS030098

Michele, B. (2020). Buckling analysis of three-phase CNT/polymer/fiber functionally graded orthotropic plates: Influence of the non-uniform distribution of the oriented fibers on the critical load. *Engineering Structures, 223*, Article 111176. https://doi.org/10.1016/j.engstruct.2020.111176

Mine, U. U., & Uğur, G. (2020). Buckling of functional graded polymeric sandwich panel under different load cases. *Composite Structures, 21*, 182-196. https://doi.org/10.1016/j.compstruct.2014.11.012

Moleiro, F., Madeira, J. F. A., Carrera, E., & Reddy, J. N. (2020). Design optimization of functionally graded plates under thermo-mechanical loadings to minimize stress, deformation and mass. *Composite Structures, 245*, Article 112360. https://doi.org/10.1016/j.compstruct.2020.112360

Mrinal, G., & Manish, C. (2021). Optimization of functionally graded material under thermal stresses. *Materials Today: Proceedings, 44*(1), 1520-1523. https://doi.org/10.1016/j.matpr.2020.11.733

Nguyen, N. V., Nguyen, X. H., Lee, D., & Lee, J. (2020). A novel computational approach to functionally graded porous plates with graphene platelets reinforcement. *Thin-Walled Structures, 150*, Article 106684. https://doi.org/10.1016/j.tws.2020.106684

Nikbakht, S., Kamarian, S., & Shakeri, M. (2019). A review on optimization of composite structures Part II: Functionally graded materials, *Composite Structures, 214*, 83-102. https://doi.org/10.1016/j.compstruct.2019.01.105

Nuttawit, W., & Arisara, C. (2015). Flexural vibration of imperfect functionally graded beams based on Timoshenko beam theory, Chebyshev collocation method. *Meccanica, 50*, 1331-1342. https://doi.org/10.1007/s11012-014-0094-8.

Phi, L. T. M., Nguyen, T. T., & Lee, J. (2021). Buckling analysis of open-section beams with thin-walled functionally graded materials along the contour direction. *European Journal of Mechanics-A/Solids, 88*, Article 104217. https://doi.org/10.1016/j.euromechsol.2021.104217

Sadiq, S. E., Bakhy, S. H., & Muhsin, J. J. (2021). Optimum vibration characteristics for honeycomb sandwich panel used in aircraft structure. *Journal of Engineering Science and Technology, 16*(2), 1463-1479.

Singh, S. J., & Harsha, S. P. (2020). Thermo-mechanical analysis of porous sandwich S-FGM plate for different boundary conditions using Galerkin Vlasov's method: a semi-analytical approach. *Thin-Walled Structures, 150*, Article 106668. https://doi.org/10.1016/j.tws.2020.106668

Thang, T. P., Nguyen, T. T., & Lee, J. (2020). Shape and material optimization for buckling behavior of functionally graded toroidal shells. *Thin-Walled Structures, 157*, Article 107129. https://doi.org/10.1016/j.tws.2020.107129

Vuong, N. V. D., & Chin, H. L. (2018). Numerical investigation on post-buckling behavior of FGM sandwich plates subjected to in-plane mechanical compression. *Ocean Engineering, 170*, 20-42. https://doi.org/10.1016/j.oceaneng.2018.10.007

Vyacheslav, N. B., & Tomasz, S. (2020). Free vibrations and static analysis of functionally graded sandwich plates with three-dimensional finite elements. *Meccanica, 55*, 815-832. https://doi.org/10.1007/s11012-019-01001-7

Wang, C., Yu, T., Shao, G., & Bui, T. Q. (2021). Multi-objective isogeometric integrated optimization for shape control of piezoelectric functionally graded plates. *Computer Methods in Applied Mechanics and Engineering, 377*, Article 113698. https://doi.org/10.1016/j.cma.2021.113698

Wang, J. F., Cao, S. H., & Zhang, W. (2021). Thermal vibration and buckling analysis of functionally graded carbon nanotube reinforced composite quadrilateral plate. *European Journal of Mechanics - A/Solids, 85*, Article 104105. https://doi.org/10.1016/j.euromechsol.2020.104105

Yassir, S., Khadija, M., Oussama, B., & Hassan, R. (2021) Buckling and post-buckling analysis of a functionally graded material (FGM) plate by the Asymptotic Numerical Method. *Structures, 31*, 1031-1040. https://doi.org/10.1016/j.istruc.2021.01.100

Yi, B., Zhou, Y., Yoon, G. H., & Saitou, K. (2019). Topology optimization of functionally-graded lattice structures with buckling constraints. *Computer Methods in Applied Mechanics and Engineering, 354*, 593-619. https://doi.org/10.1016/j.cma.2019.05.055

Zhao, J., Zhang, M., Zhu, Y., Li, X., Wang, L., & Hu, J. (2019). A novel optimization design method of additive manufacturing-oriented porous structures and experimental validation. *Materials & Design*, *163*, Article 107550. https://doi.org/10.1016/j.matdes.2018.107550

Zhu, F., Wang, Z., Lu, G., & Zhao, L. (2009). Analytical investigation and optimal design of sandwich panels subjected to shock loading. *Materials & Design, 30*(1), 91-100. https://doi.org/10.1016/j.matdes.2008.04.027